Band alignment at a nonplanar Si/SiO_2 interface

K. Seino* and F. Bechstedt
Institut für Festkörpertheorie und-optik, Friedrich-Schiller-Universität Jena, Max-Wien-Platz 1, 07743 Jena, Germany

P. Kroll
Department of Chemistry and Biochemistry, The University of Texas at Arlington, Arlington, Texas 76019, USA
(Received 29 April 2010; revised manuscript received 5 August 2010; published 19 August 2010)

The interfacial electronic properties of silicon nanocrystals embedded in a silica matrix are studied using *ab initio* density-functional theory. We aim to obtain local band edges for a typical nanostructured system, nanocrystals embedded in a surrounding matrix. We compute the spatial variation in the electronic structure for realistic Si nanocrystals with nominal diameters ranging between 0.8 and 1.6 nm, i.e., up to systems with more than 1000 atoms. The evolution of the valence and conduction band edges between Si nanocrystals and amorphous silica along radial directions versus size is presented. Significant differences are found comparing embedded Si nanocrystals and planar Si/SiO_2 interfaces.

DOI: 10.1103/PhysRevB.82.085320 PACS number(s): 73.20.−r, 73.22.−f, 78.67.Bf

I. INTRODUCTION

Nanoscale semiconductor structures exhibit new physical properties. For example, effects due to spatial quantization of electrons and holes help to overcome the limitation of the indirect-gap semiconductor Si for light emission by breaking the **k**-selection rule. Si nanocrystals (NCs) embedded in an insulating matrix, most often amorphous silica (a-SiO_2), represent the most prevalent nanoscale silicon systems.[1–4] Samples with Si NCs embedded in SiO_2 have been fabricated using a variety of deposition techniques[5–7] or annealing of SiO_x/SiO_2 superlattices.[8–10] Size-controlled NC synthesis is now possible.[8,11] In particular, the confinement influence on the fundamental gaps and its size dependence have widely been studied. However, still the origin of the quantum confinement, its possible modification due to an embedding matrix, as well as its consequence for NC applications are under debate.

Simulation is a powerful tool for investigating and understanding atomic-scale phenomena and interpreting experiments. Theoretical studies of properties for Si NCs embedded in SiO_2 are, however, computationally challenging, because these systems are rather large and their atomic geometries are relatively complex. Several computational attempts for Si NCs embedded in SiO_2 have been performed.[6,12–20] Studies using empirical methods such as a Monte Carlo (MC) approach or molecular dynamics[12–17] have improved the understanding of the interface structure for embedded Si NCs. First-principles calculations based on the density-functional theory (DFT) have been used to study electronic and optical properties for Si NCs inserted into a SiO_2 matrix.[6,14,18–20] However, earlier work[6] was restricted to too small and unrealistic NCs. Recently, realistic atomic geometries have been derived within full quantum-mechanical modeling.[21–23]

The key property is the Si/SiO_2 interface. It constitutes a barrier for carrier (electron or hole) transport from cluster to the amorphous matrix. The discontinuities of conduction and valence band edges between Si and SiO_2 are the relevant parameters for barrier characterization. A well-investigated system is the planar $Si(100)/SiO_2$ interface. First-principles calculations have been performed to obtain the spatial profiles of local band edges, local band gaps as well as their band offsets through the interface in normal direction.[24–29] Unfortunately, knowledge gained from studies of planar Si/SiO_2 interfaces cannot be transferred to interfacial properties of Si NCs embedded in SiO_2 matrices, because clusters exhibit a variety of facets, displaying several crystallographic orientations. Therefore, simplistic planar interface models adopted to match ideal β cristobalite to the Si(100) interface[30] are not suitable to describe curved interfaces of Si NCs.

In this paper we focus on the interfacial electronic properties of Si nanocrystals embedded in an amorphous SiO_2 matrix for various dot sizes by means of parameter-free first-principles calculations. The local electronic properties, especially the position of the band edges, are investigated for defect-free interfaces which represent minimum total-energy atomic geometries. The consequences of dimensional and size effects are discussed for local band discontinuities between nanocrystals and matrix.

II. COMPUTATIONAL METHODS

First-principles calculations are performed using the Vienna *ab initio* simulation package (VASP) implementation[31] of the DFT (Ref. 32) within local-density approximation (LDA).[33] The electron-ion interaction is described within the projector augmented-wave method.[34] The supercell approach is applied in order to use a plane-wave expansion of the eigenfunctions. The kinetic cutoff energy of plane-wave expansion is taken to be 400 eV. The Brillouin-zone integrations are carried out using only the Γ point. The atomic structure of embedded NCs in a SiO_2 matrix is considered to be in equilibrium when the Hellmann-Feynman forces are smaller than 0.1 eV/Å.

In this paper we study Si NCs in vitreous silica. The structure models have been generated using combinations of a network switching algorithm and the DFT method. The details of the geometry constructions are described in Refs. 21 and 22. In cubic supercells filled with Si atoms the core of

 ©2010 The American Physical Society

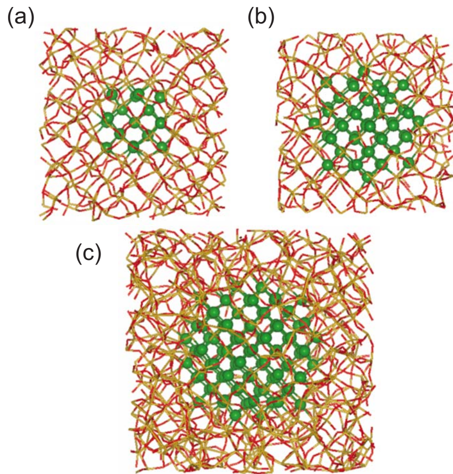

FIG. 1. (Color online) Model of a Si NCs embedded in SiO_2 with various diameters of (a) 0.8 nm, (b) 1.2 nm, and (c) 1.6 nm. The Si atoms in the core are indicated by green dots. Si-Si and Si-O bond are represented by solid lines.

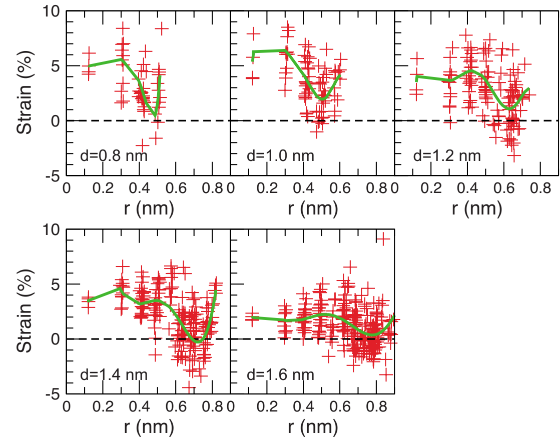

FIG. 2. (Color online) Bond-length strain as a function of the distance r of the center of the bond from the center of the NC for various nominal NC diameters d. The dashed line at zero corresponds to the bulk bond length. The solid (green) lines give the averages.

the Si NC is defined by a certain diameter. The nominal diameter of the Si cores d varies in the range of 0.8, 1.0, 1.2, 1.4, and 1.6 nm. The O atoms are inserted between pairs of Si atoms outside the core. Starting from a resulting atomic geometry the topology of the SiO_2 network is randomized by means of a bond switching algorithm. Using the network switching algorithm with the flavor of the Wooten-Waire-Winer algorithm,[35] a realistic model for amorphous SiO_2 is provided. Our procedure for amorphous SiO_2 structures is almost identical to the approach of a previous treatment with the MC method by Hadjisavvas and Kelires.[12] Subsequent to the empirical network method, we optimize the atomic positions in the resulting spherical embedded NCs using the first-principles calculations within DFT-LDA.

Models with Si NCs up to 1.2 nm are constructed applying a $3\times3\times3$ supercell of diamond. They contain 500–600 atoms. Models with larger embedded Si NCs originate from a $4\times4\times4$ supercell and comprise more than 1000 atoms. All interface bonds remain intact: Si atoms are fourfold coordinated while O atoms are twofold coordinated without any O-O bonds. Figure 1 shows the geometries of Si NCs embedded in a-SiO_2 with diameters of 0.8, 1.2, and 1.6 nm which have been obtained after complete ionic relaxation.

III. RESULTS AND DISCUSSION

A. Structural, elastic, and electronic properties

In Fig. 2 we show the distribution of the strain in the Si core regions as function of the distance from the center. It is defined as bond-length strain, i.e., the relative deviation of a Si-Si bond length with respected to its bulk value. The average of Si–Si bond lengths for Si NCs embedded in SiO_2 is larger than that for the bulk Si (2.34 Å, DFT-LDA). Many of Si-Si bonds have a larger bond length than the bulk value. Only near the Si nanocrystal/SiO_2 matrix interfaces shorter Si-Si bonds appear. The strain distributions in Fig. 2 illustrate a tendency of a tensile strain at Si-Si bonds in the NC core. Near the interface a compressive strain is also visible for certain bonds.

Similarly, an expansion of the material inside the NC has also been found for isolated hydrogenated Si NCs.[36] For hydrogenated NCs Weissker *et al.*[36] reported that the bond lengths are longest near the center of the NC, in general, and decrease toward their surface. However, the plot in Fig. 2 shows a more complex behavior, especially in the interface region. This is the consequence of a matrix influence for embedded Si NCs.

Our results for the bond-length distribution are seemingly in contrast to those of the molecular dynamics simulations by Yilmaz *et al.*[17] They also found stretched bonds in the Si core but only of the order of 1%. The smaller average value of 1% is probably a consequence of the larger diameter of $d=3.2$ nm of the studied Si NCs. A tendency of the reduction of tensile strain with increasing diameter is demonstrated in Fig. 2. However, in the interface region Yilmaz *et al.*[17] observed a general stretching of the Si-Si bonds in contrast to the present findings. We observe stretched and shortened bonds. In the average they decrease toward the nominal NC radius $r=d/2$ and increase slightly for the interface regions $r>d/2$. The reason may be the fact that the used classical interaction potentials do not correctly describe the effect of the ionic bonding in contrast to our full quantum-mechanical optimization of the interface geometries. Another reason may be the larger NC diameter in Ref. 17.

The averaged values for bond lengths and bond angles in the oxide are given in Table I. The parameters are characterized for the interface and matrix regions. The averages of the Si-O bond lengths are not very different for interface and matrix regions. The average values for the Si-O bond lengths for the interface regions are slightly larger than those in the matrix regions for all diameters. The deviations are small in both matrix and interface regions. The averages of the bridge angles at the oxygen atoms, namely the Si-O-Si bond angles, are between 140° and 146°. Our average results are close to the values 1.62 Å and $136\pm14°$ discussed for bulk amorphous SiO_2 networks[37] or close to Si-O-Si angles of vitreous

TABLE I. Mean (μ) and standard deviation (σ) of the distributions of bond lengths and bond angles in the interface and the oxide matrix for five different NCs characterized by the diameter d.

	Si-O (Å)				∠Si-O-Si (deg)				∠O-Si-O (deg)			
d	Interface		Matrix		Interface		Matrix		Interface		Matrix	
(nm)	μ	σ	μ	σ	μ	σ	μ	σ	μ	σ	μ	σ
0.8	1.63	0.01	1.61	0.01	146.5	12.7	144.6	13.1	105.5	4.9	109.5	3.3
1.0	1.63	0.01	1.61	0.01	143.5	14.8	141.5	12.6	105.9	5.3	109.5	3.9
1.2	1.62	0.01	1.61	0.01	142.4	14.0	140.0	15.2	106.4	4.9	109.5	4.3
1.4	1.61	0.02	1.60	0.02	142.6	13.5	141.8	13.4	106.4	5.3	109.5	3.8
1.6	1.61	0.02	1.60	0.02	144.4	13.3	143.9	13.2	106.9	4.8	109.5	4.0

silica.[38] However, the variation around the average values of about 13°–15° is rather large in interface and matrix. The tetrahedron angles in the SiO_4 tetrahedra, i.e., the O-Si-O bond angles, are almost preserved in the matrix at the ideal value. Only in the interface region a drastic reduction is clearly visible. Similar values are obtained for the system of a planar $Si(100)/SiO_2$ interface.[39]

To characterize the interface more from the point of electrostatics and number of oxygen neighbors of Si atoms, we classify the Si atoms in different charge states between 0 and 4. Their distribution versus the distance to the NC center is shown in Fig. 3 for embedded NCs of different diameters. For all cases almost all suboxide species exist in the interface

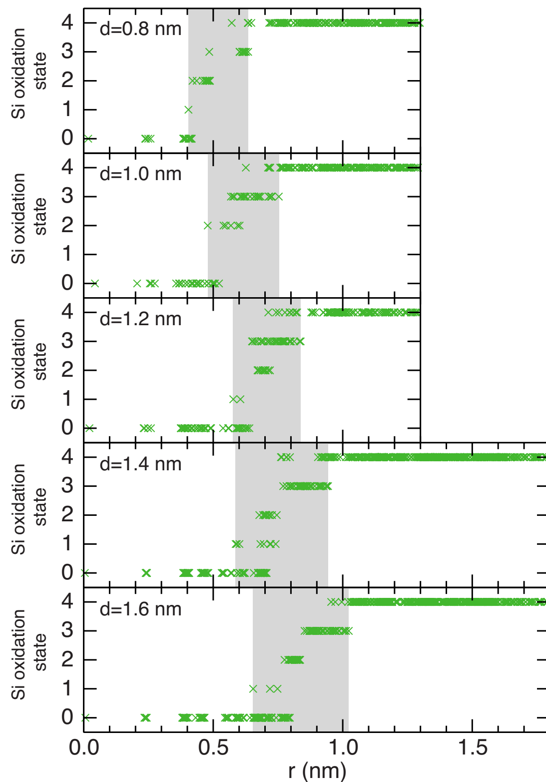

FIG. 3. (Color online) Distribution of Si atoms Si^{0+}, Si^{1+}, Si^{2+}, Si^{3+}, and Si^{4+} in different charge states versus distance r to the NC center. The interface regions are shaded.

region of the systems shown in Fig. 3. Their distribution and transition into the core region with neutral Si atoms, Si^{0+}, and the matrix with fully ionized Si atoms, Si^{4+}, allow the definition of an interface region and extent, respectively. The interface regions are illustrated in Fig. 3 by gray shadows and have a range between 0.2 and 0.4 nm. These values are in excellent agreement with suboxide thicknesses derived from x-ray spectroscopy.[10] It has been reported that the suboxide densities are dependent on NC size.[7] The suboxide distributions in Fig. 3 confirm such a dependence and show a monotonous increase in the charge state through the interface. Thereby, a low probability of the charge state Si^{1+} is obvious. For the small NC sizes, the low probability of the charge state Si^{1+} is also observed from core-level photoemission data for slightly larger NC diameters.[7] The finding of a suppressed Si^{1+} probability is not due to the network switching algorithm. The bond switching algorithm leaves the distribution of oxidation states fixed. The algorithm does not touch a Si-Si bond. It neither breaks it nor inserts an O atom into it.

The spatial variation in the different charge states in Fig. 3 shows similarities with the behavior for the planar $Si(100)/SiO_2$ interface.[25] However, there are three striking differences: (i) in the three-dimensional nonplanar, i.e., curved Si nanocrystal/SiO_2 matrix interface the probability to find the charge state Si^{1+} is relatively low. (ii) There is a much stronger overlap of the regions for which different charge states can simultaneously occur. (iii) The interface extent, i.e., the region of Si suboxides, is smaller than the value of 0.6 nm estimated for the planar interface.

B. Band-edge profiles

In order to discuss the band-edge profiles through the nanocrystal-matrix system we calculate the density of states (DOS), focusing on local site-projected properties. The procedure to obtain the local band-edge profiles is as follows: first we calculate a site-projected density of state (pDOS). Then we determine local band edges from the site-projected DOS according to a method described well for planar Si/SiO_2 systems.[24] One derives the corresponding quantities for each Si and O atom. Each atom onto which the DOS is projected possesses a certain distance r from the NC center.

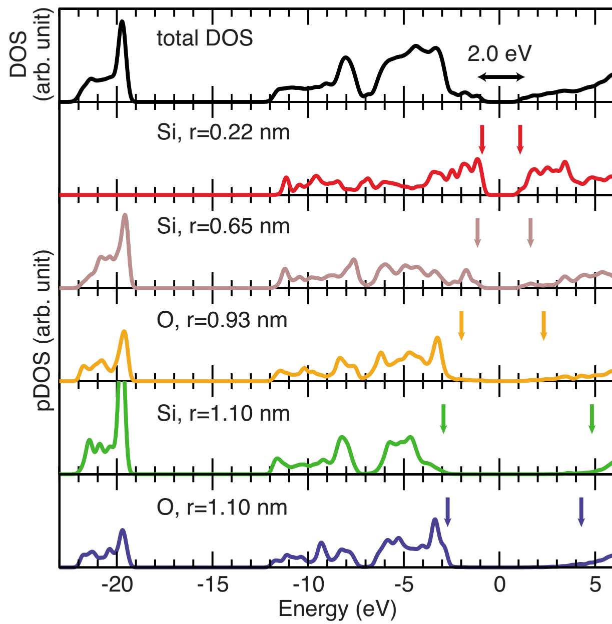

FIG. 4. (Color online) Calculated DOS and pDOS for several Si and O atoms of an embedded NC with diameter $d=1.2$ nm. r is the atom distance from the NC center. The energy zero is the middle of the energy gap. The band edges are marked by arrows.

An illustration is given in Fig. 4 for atoms of different nature and position. It shows the pDOS for projections onto Si and O atoms with different distance r to the NC center: A Si atom close to the center ($r=0.22$ nm), interface atoms ($r=0.65$ nm and 0.93 nm for Si and O atoms, respectively), and Si and O atoms in the matrix region ($r=1.10$ nm). A Gaussian broadening of 0.1 eV is applied for the analysis of the total DOS and pDOS.

Calculated pDOSs of Si and O atoms show a different behavior for the three spatial regions, near the center, in the interface, and in the host matrix. The densities around the gap are not only dominated by core Si atoms but also by contributions of Si atoms belonging to the suboxide in the interface. In the interface region, the feature that the highest valence and lowest conduction states are determined by Si states still persists. However, the contribution of O states also plays a role. In the matrix region, the local band gaps are larger than those in the core and interface regions for both Si- and O-projected DOSs. The orbital character of the uppermost valence states depends mostly on the atomic position. Core Si atoms contribute with $3p$ and $3s$ states, whereas contributions of O $2p$ and Si $3p$ states dominate the pDOS in the SiO_2 matrix.

The resulting evolution of the local band edges is plotted as a function of the distance from the center for various NC sizes in Fig. 5. Within the core regions the positions of the band edges are practically independent of the atomic position. The distance of the band edges are virtually identical with the fundamental band gaps in the core region.[23] A similar behavior is observed for the SiO_2 matrix region. The distances between the highest occupied and lowest empty band edges represent the energy gap of the SiO_2 matrix material rather independent of the NC diameter.

The interface region is indicated by the significant variation in the band edges. Figure 5 shows a spatial overlap of band-edge positions for Si atoms. The interface region is seemingly ~0.4 nm more distant from the NC center as expected from the definition of the NC radius in the construction as average distance of the Si atoms in the uppermost NC shell to the center. Because of the transition region the effective NC diameters d_{eff} have to be increased by about 0.4 nm with respect to d. This value is slightly smaller than obtained by classical calculations[12] or experiment.[6] However, Fig. 5 also indicates that a precise definition of the interface region is difficult. Taking further weak spatial variations in the band edges into account, larger extents up to 0.7–0.8 nm can be predicted. The comparison of the results in Figs. 3 and 5 indicates that the average position of the almost spherical interface as well as its matrix depends on the system property studied.

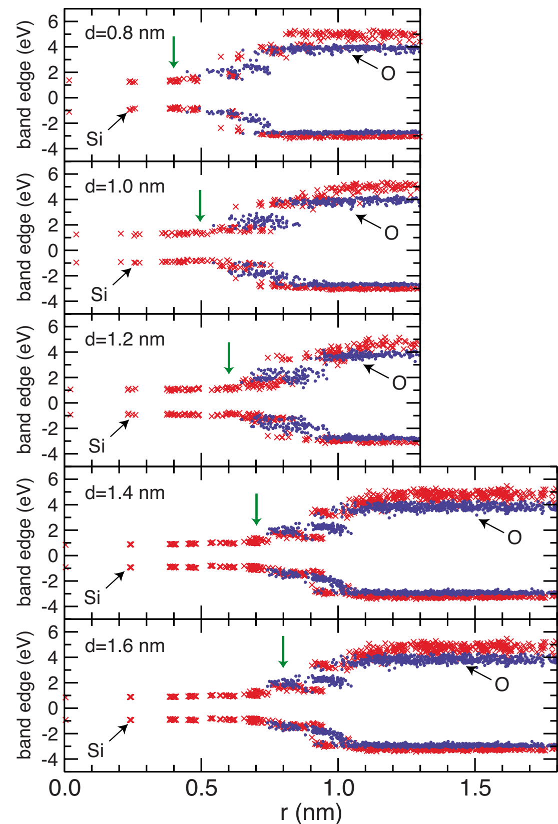

FIG. 5. (Color online) Profiles of the band edges as a function of the distance r from the NC center for various NC sizes. Projections onto different atoms, Si (crosses, red) and O (circles, blue), are plotted. The different extents of the SiO_2 matrix are due to the use of two different supercell sizes. The vertical arrow indicates the nominal NC size.

The spatial variation in the band edges in Fig. 5 is correlated with the distribution of partially oxidized Si atoms in different charge states according to the number of highly ionic Si-O bonds of a particular Si atom in Fig. 3. The overlap regions of Si- and SiO_2-like band edges in Fig. 5 widely agree with the radius ranges in which Si^{1+}, Si^{2+}, and Si^{3+} occur in Fig. 3. These ranges give smaller measures of the interface extent of about 0.25 nm (small NCs) or 0.35 nm (large NCs) with respect to the distribution of the charge states.

TABLE II. Averaged local band gaps of Si NCs ($\bar{E}_g^{NC}$) and SiO_2 ($\bar{E}_g^{SiO_2}$), reduced band offsets (VBO and CBO) for various NC diameters *d*. The values due to projection only onto Si atoms are given in parentheses.

d (nm)	$\bar{E}_g^{NC}$ (eV)	$\bar{E}_g^{SiO_2}$ (eV)	VBO (eV)	CBO (eV)
0.8	2.2	6.6 (7.9)	1.9 (2.1)	2.5 (3.6)
1.0	2.2	6.6 (7.9)	1.8 (2.1)	2.6 (3.6)
1.2	2.0	6.6 (7.7)	1.9 (2.2)	2.7 (3.6)
1.4	1.9	6.7 (8.0)	2.0 (2.3)	2.8 (3.8)
1.6	1.8	6.6 (7.8)	2.2 (2.5)	2.7 (3.5)

The averaged values of the local band gaps in the Si NCs $\bar{E}_g^{NC}$ and in the SiO_2 matrix $\bar{E}_g^{SiO_2}$ are listed in Table II. The smaller values are due to projection onto O atoms while the larger ones are related to projections onto Si atoms of the matrix. The local band gaps at the Si core $\bar{E}_g^{NC}$ reproduce the highest occupied molecular orbital-lowest unoccupied molecular orbital gaps for Si NCs embedded in SiO_2.[23] As we have reported in Ref. 23, the quantum confinement effects are also visible for Si NCs embedded in SiO_2. The increase in $\bar{E}_g^{NC}$ with respect to the Si bulk value in the core region is mainly due to the confinement of the holes in agreement with experimental findings.[2,10] The gap energies $\bar{E}_g^{NC}$ are significantly larger than the gap energies for Si/SiO_2 structures with planar interfaces which amount to about $0.5 \sim 1.0$ eV within DFT-LDA (Refs. 30 and 40) while the value of bulk Si is $E_g^{bulk}=0.44$ eV. However, the gap values for embedded NCs are smaller than that for hydrogenated NCs.[30] On the other hand, the values $\bar{E}_g^{SiO_2}$ remain almost constant and uninfluenced by confinement effects.

The DFT-LDA underestimates the quasiparticle energy gaps of semiconductor materials.[41] Such an underestimation of the energy gaps within DFT-LDA also influences the results in Fig. 3 and Table II. Since DFT-LDA is a ground-state theory, its electronic energy eigenvalues do not correctly describe the excitation energies of electrons and holes. For instance, the bulk Si value of the fundamental indirect gap is found as 0.44 eV. Including many-body quasiparticle effects[41,42] the correct experimental value is, however, nearly obtained. In systems with strong quantum confinement one can include the Coulomb interaction of quasielectrons and quasiholes in the pair excitation energies by means of the delta-self-consistent-field (ΔSCF) method.[43] However, this method yields optical gaps instead quasiparticle ones. The pair excitation energies from the ΔSCF method including many-body effects are only slightly larger than the results from DFT-LDA.[23] The optical gaps including electron-hole interaction are almost correctly described for hydrogenated and embedded Si NCs due to compensation of quasiparticle and excitonic effects.[23,43] This is also expected for the embedded NCs. In the past quasiparticle corrections have also been computed for the optical transitions in SiO_2.[44] Quasiparticle corrections have also been calculated for Si/SiO_2 multiple quantum well structures.[30] From these findings we conclude that the underestimation of the minimum matrix gaps is due to the DFT-LDA, which usually leads to underestimated quasiparticle band gaps, also for bulk SiO_2.[45] Consequently, the corresponding quasiparticle band gaps in Fig. 5 in the SiO_2 matrix region should be larger by a quasiparticle shift of about 2 eV while their values in the Si core region are less influenced due to the relatively strong confinement effects.

The differences between the local band edges in the Si core and SiO_2 matrix regions in Fig. 5 may be interpreted to be the valence-band offsets (VBOs) and conduction-band offsets (CBOs) at the Si nanocrystal/SiO_2 matrix interface, respectively. In order to determine the band offsets, we here use the positions of Si- and/or O-related band edges according to the method described in Refs. 25 and 46. These quantities are not identical with the valence or conduction band discontinuities (VBD or CBD) between two bulk materials for which a well-defined calculation procedure by Van de Walle and Martin[47] exists, at least for planar and almost lattice-matched interfaces between crystalline nonmetals. The main difference is that the band offsets VBO and CBO are reduced by the confinement energies of holes or electrons in the NC. These reduced band offsets are also summarized in Table II. The VBOs increase slightly with increasing NC diameter *d*. Within the applied framework of approaches the CBOs seem to be almost constant versus the NC diameter. The NC gap variation is mainly built up by the VBO.

The values of the resulting gaps and band offsets have to be compared with those obtained for planar Si/SiO_2 interfaces. The calculated Si NC band gaps between 1.8 and 2.2 eV are larger than the DFT-LDA values 0.6–1 eV derived for layered Si nanostructures with planar Si/SiO_2 interfaces.[24,25,29] The confinement effects in embedded Si NCs are stronger than in planar Si/SiO_2 heterostructures. The magnitude of the band offsets in Table II is smaller than band discontinuities calculated for planar Si/SiO_2 interfaces[24–27,29] or measured ones of about 4.3 eV (VBD) and 3.1 eV (CBD) (Refs. 48 and 49) especially for projections onto O atoms in SiO_2. However, the difference between the reduced band offsets in Table II and VBDs and CBDs to those for planar interfaces cannot solely be traced back to different confinements due to dimensionality or electron and hole masses. Rather, it seems to be related to the occurrence of interfaces in all space directions, which do not allow an interface-induced electric dipole for the NC system for symmetry reasons. This fact leads to modified relative band-edge positions between planar and nonplanar interfaces. In addition, the three-dimensional confinement can more act on hole states and hence stronger decreases the band offsets between the valence states in Si and SiO_2. The underestimation of the band gaps from DFT-LDA may also lead to reduced band discontinuities. However, the quasiparticle effects should not give rise to much more increased VBOs in comparison with the CBOs so that the relation of VBO $<$ CBO is observed in contrast relation VBD $>$ CBD for planar Si/SiO_2 structures.

Recently, the band alignment between Si NCs and almost lattice-matched Gd_2O_3 is reported.[50] Unfortunately, the results cannot directly be compared with our results because the matrix material is different. The band gap measured for the smallest NCs with 3 nm diameter amounts to 2.9 eV,

which is much larger than the values calculated for Si NCs embedded in SiO_2. The CBD between Si NCs and lattice-matched Gd_2O_3 seems to be smaller than that for the planar Si/SiO_2 interfaces.[48,49] More detail discussions ask for further experiments. This holds especially for the relative large gap measured for 3 nm NCs.

The profiles of the local band edges in Fig. 5 can roughly be identified with the confinement potentials acting on electrons or holes used in the effective-mass approximation. Ignoring the extent of the interface regions these potentials can be approximated as those of a three-dimensional rectangular potential well with a well depth of CBO or VBO from Table II. However, Fig. 5 also indicates that in the interface regions $d/2 < r < d/2+0.4$ nm the spatial variations in the band edges are far away from discontinuities. There are smoother variations with significantly reduced offsets near $r \approx d/2+0.2$ nm. These deviations from a sharp interface and abrupt confinement potentials may explain why first-principles calculations[23] give rise to a diameter variation d^{-n} of the NC energy gaps with values $n < 2$ expected for rectangular potential wells and effective-mass particles ($n=0.6-0.8$ from experiments[9] and $n=0.48$ from calculations[23]).

IV. CONCLUSION

We have studied the bonding and electronic properties at the interface of Si nanocrystals embedded in a-SiO_2. The Si-Si bonds in the nanocrystal core are stretched while in the interface regions both types of bonds, stretched and compressed ones, occur. The local band edge profiles exhibit different band gaps in the Si nanocrystals and in the matrix region. The calculated results show deviations from the behavior of the planar Si/SiO_2 interface, a modified relative band alignment and three-dimensional confinement effects, which are stronger for valence states and hence holes. The band-edge profiles are correlated with the distribution of Si atoms in the different charge states. However, the interface extent defined by the charge state distribution and the local band profiles differ slightly. In any case, they indicate that the true nanocrystals are somewhat more extended than the nominal Si core, although the extent depends on the actual interface studied.

ACKNOWLEDGMENTS

This work was supported by the BMBF, Germany (Projects Nos. 03SF0352D and 13N9669). P.K. was supported by the NSF (Grant No. DMR-0907117). Grants of computer time from John von Neumann Institute for Computing (NIC) in Jülich, from UTA-HPC, and from the Texas Advanced Computing Center (TACC) in Austin, TX, are gratefully acknowledged.

*seino@ifto.physik.uni-jena.de

[1] L. Pavesi, L. D. Negro, C. Mazzoleni, G. Franzò, and F. Priolo, Nature (London) **408**, 440 (2000).

[2] M. V. Wolkin, J. Jorne, P. M. Fauchet, G. Allan, and C. Delerue, Phys. Rev. Lett. **82**, 197 (1999).

[3] S. Godefroo, M. Hayne, M. Jivanescu, A. Stesmans, M. Zacharias, O. I. Lebedev, G. van Tendeloo, and V. V. Moshchalkov, Nat. Nanotechnol. **3**, 174 (2008).

[4] I. Perez-Wurfl, X. Hao, A. Gentle, D. H. Kim, G. Conibeer, and M. A. Green, Appl. Phys. Lett. **95**, 153506 (2009).

[5] V. Vinciguerra, G. Franzo, F. Priolo, F. Iacona, and C. Spinella, J. Appl. Phys. **87**, 8165 (2000).

[6] N. Daldosso, M. Luppi, S. Ossicini, E. Degoli, R. Magri, G. Dalba, P. Fornasini, R. Grisenti, F. Rocca, L. Pavesi, S. Boninelli, F. Priolo, C. Spinella, and F. Iacona, Phys. Rev. B **68**, 085327 (2003).

[7] S. Kim, M. C. Kim, S.-H. Choi, K. J. Kim, H. N. Hwang, and C. C. Hwang, Appl. Phys. Lett. **91**, 103113 (2007).

[8] M. Zacharias, J. Heitmann, R. Scholz, U. Kahler, M. Schmidt, and J. Bläsing, Appl. Phys. Lett. **80**, 661 (2002).

[9] J. Heitmann, F. Müller, L. Yi, M. Zacharias, D. Kovalev, and F. Eichhorn, Phys. Rev. B **69**, 195309 (2004).

[10] A. Zimina, S. Eisebitt, W. Eberhardt, J. Heitmann, and M. Zacharias, Appl. Phys. Lett. **88**, 163103 (2006).

[11] J. Heitmann, F. Müller, M. Zacharias, and U. Gösele, Adv. Mater. **17**, 795 (2005).

[12] G. Hadjisavvas and P. C. Kelires, Phys. Rev. Lett. **93**, 226104 (2004).

[13] G. Hadjisavvas, I. N. Remediakis, and P. C. Kelires, Phys. Rev. B **74**, 165419 (2006).

[14] G. Hadjisavvas and P. Kelires, Physica E **38**, 99 (2007).

[15] L. T. Kong and L. J. Lewis, Phys. Rev. B **77**, 085204 (2008).

[16] F. Djurabekova and K. Nordlund, Phys. Rev. B **77**, 115325 (2008); D. Flyura, B. Marie, and N. Kai, Nucl. Instrum. Methods Phys. Res. B **266**, 2683 (2008).

[17] D. E. Yilmaz, C. Bulutay, and T. Cagin, Phys. Rev. B **77**, 155306 (2008).

[18] M. Luppi and S. Ossicini, Phys. Rev. B **71**, 035340 (2005).

[19] N. B. Nguyen, C. Dufour, and S. Petit, J. Phys.: Condens. Matter **20**, 455209 (2008).

[20] R. Guerra, I. Marri, R. Magri, L. Martin-Samos, O. Pulci, E. Degoli, and S. Ossicini, Phys. Rev. B **79**, 155320 (2009); R. Guerra, E. Degoli, and S. Ossicini, *ibid.* **80**, 155332 (2009); R. Guerra, I. Marri, R. Magri, L. Martin-Samos, O. Pulci, E. Degoli, and S. Ossicini, Superlattices Microstruct. **46**, 246 (2009).

[21] P. Kroll and H. J. Schulte, in *Group IV Semiconductor Nanostructures-2006*, edited by C. Delerue, L. Tsybeskov, D. J. Lockwood, M. Ichikawa, and A. W. van Buure, MRS Symposia Proceeding No. 958 (Materials Research Society, Pittsburgh, 2007) pp. 0958-L07-16.

[22] P. Kroll and H. J. Schulte, Phys. Status Solidi B **243**, R47 (2006).

[23] K. Seino, F. Bechstedt, and P. Kroll, Nanotechnology **20**, 135702 (2009).

[24] T. Yamasaki, C. Kaneta, T. Uchiyama, T. Uda, and K. Terakura, Phys. Rev. B **63**, 115314 (2001).

[25] F. Giustino, A. Bongiorno, and A. Pasquarello, Jpn. J. Appl. Phys. **43**, 7895 (2004).

[26] R. Shaltaf, G.-M. Rignanese, X. Gonze, F. Giustino, and A. Pasquarello, Phys. Rev. Lett. **100**, 186401 (2008).
[27] A. Alkauskas, P. Broqvist, F. Devynck, and A. Pasquarello, Phys. Rev. Lett. **101**, 106802 (2008).
[28] S. Markov, P. V. Sushko, S. Roy, C. Fiegna, E. Sangiorgi, A. L. Shluger, and A. Asenov, Phys. Status Solidi A **205**, 1290 (2008).
[29] M. Ribeiro, L. R. C. Fonseca, and L. G. Ferreira, Phys. Rev. B **79**, 241312 (2009).
[30] K. Seino, J. M. Wagner, and F. Bechstedt, Appl. Phys. Lett. **90**, 253109 (2007).
[31] G. Kresse and J. Furthmüller, Comput. Mater. Sci. **6**, 15 (1996).
[32] P. Hohenberg and W. Kohn, Phys. Rev. **136**, B864 (1964).
[33] W. Kohn and L. J. Sham, Phys. Rev. **140**, A1133 (1965).
[34] G. Kresse and D. Joubert, Phys. Rev. B **59**, 1758 (1999).
[35] P. Kroll, J. Eur. Ceram. Soc. **25**, 163 (2005).
[36] H. C. Weissker, J. Furthmüller, and F. Bechstedt, Phys. Rev. B **67**, 245304 (2003).
[37] J. Sarnthein, A. Pasquarello, and R. Car, Phys. Rev. Lett. **74**, 4682 (1995).
[38] F. Mauri, A. Pasquarello, B. G. Pfrommer, Y.-G. Yoon, and S. G. Louie, Phys. Rev. B **62**, R4786 (2000).
[39] A. Bongiorno and A. Pasquarello, Appl. Phys. Lett. **83**, 1417 (2003).
[40] J.-M. Wagner, K. Seino, F. Bechstedt, A. Dymiati, J. Mayer, R. Rölver, M. Först, B. Berghoff, B. Spangenberg, and H. Kurz, J. Vac. Sci. Technol. A **25**, 1500 (2007).
[41] W. G. Aulbur, L. Jönsson, and J. W. Wilkins, Solid State Phys. **54**, 1 (1999).
[42] F. Fuchs, J. Furthmüller, F. Bechstedt, M. Shishkin, and G. Kresse, Phys. Rev. B **76**, 115109 (2007).
[43] H.-C. Weissker, J. Furthmüller, and F. Bechstedt, Phys. Rev. B **69**, 115310 (2004).
[44] L. E. Ramos, J. Furthmüller, and F. Bechstedt, Phys. Rev. B **69**, 085102 (2004).
[45] Y.-N. Xu and W. Y. Ching, Phys. Rev. B **44**, 11048 (1991).
[46] F. Devynck, F. Giustino, P. Broqvist, and A. Pasquarello, Phys. Rev. B **76**, 075351 (2007).
[47] C. G. Van de Walle and R. M. Martin, Phys. Rev. B **34**, 5621 (1986).
[48] J. W. Keister, J. E. Rowe, J. J. Kolodziej, H. Niimi, T. E. Madey, and G. Lucovsky, J. Vac. Sci. Technol. B **17**, 1831 (1999).
[49] V. V. Afanas'ev, M. Houssa, A. Stesmans, and M. M. Heyns, Appl. Phys. Lett. **78**, 3073 (2001).
[50] V. V. Afanas'ev, M. Badylevich, A. Stesmans, A. Laha, H. J. Osten, and A. Fissel, Appl. Phys. Lett. **95**, 102107 (2009).